A Quantum Cascade Laser–Based Reflectometer for On-Orbit Blackbody Cavity Monitoring

P. JONATHAN GERO

Space Science and Engineering Center, University of Wisconsin—Madison, Madison, Wisconsin

JOHN A. DYKEMA AND JAMES G. ANDERSON

School of Engineering and Applied Sciences, Harvard University, Cambridge, Massachusetts

(Manuscript received 15 September 2008, in final form 13 March 2009)

ABSTRACT

Satellite measurements pinned to international standards are needed to monitor the earth's climate, quantify human influence thereon, and test forecasts of future climate change. Credible observations require that measurement uncertainties be evaluated on orbit during a mission's operational lifetime. The most accurate spaceborne measurements of thermal infrared radiance are achieved with blackbody calibration. The physical properties of blackbody cavity surface coatings are known to change upon extended exposure to the low earth orbit environment. Any such drift must be quantified to continue correctly calibrating observed radiance on orbit. A method is presented to diagnose the effective emissivity of a blackbody cavity in situ using a quantum cascade laser (QCL)-based reflectometer. QCLs provide high-power single-mode output in the thermal infrared and have small mechanical footprints that facilitate integration into existing optical systems. The laser reflectivity in a test blackbody cavity was measured to be 9.22×10^{-4} with an uncertainty of 8.9×10^{-5}, which is equivalent to a detection limit of 3 mK in the error in radiance temperature for a calibration blackbody (at 330 K and 1000 cm^{-1}) resulting from cavity emissivity drift. These results provide the experimental foundation for this technology to be implemented on satellite instruments and thus eliminate a key time-dependent systematic error from future measurements on orbit.

1. Introduction

Measurements of spectral infrared radiance from space are an effective benchmark of global climate change if they are made with demonstrable on-orbit accuracy. A time series of spectrally resolved thermal infrared radiance emitted from the earth to space contains signatures of the longwave forcing of the climate, the climate's response, and the longwave feedbacks inherent in that response and therefore establishes a high-accuracy record of climate change and also provides powerful constraints on climate models. The timely detection of decadal climate signals above natural variability requires measurements with a high level of accuracy (Leroy et al. 2008). Recent studies (Anderson et al. 2004; National Research Council 2007; Ohring 2008) call for measurements of thermal infrared radiance with uncertainties better than 0.1 K (3σ) in radiance temperature for the detection of spectral climate signatures. This level of uncertainty, proven on orbit, has not yet been accomplished by space-based high-resolution infrared sounders.

The determination of satellite sensor uncertainty during prelaunch calibration cannot be assumed to be valid over the operational lifetime of the instrument. The harsh conditions of spacecraft launch and the low earth orbit environment can lead to secular drifts in instrument physical properties that are manifest as a time-dependent bias in the absolute calibration. Degradation affecting blackbodies, which provide the fundamental radiometric calibration for spaceborne infrared sounders, is a particular concern. Unequivocal demonstration of adequate instrument uncertainty levels on orbit necessitates traceability to the International System of Units (SI). The SI units are linked to fundamental physical properties of matter and can be realized anywhere in the world

Corresponding author address: Dr. P. Jonathan Gero, Space Science and Engineering Center, University of Wisconsin—Madison, 1225 W. Dayton St., Madison, WI 53706.
E-mail: jonathan.gero@ssec.wisc.edu

DOI: 10.1175/2009JTECHA1227.1

without bias. By doing so, one can make an absolute measurement to within a specified uncertainty. For a satellite instrument, SI traceability can be achieved by tying the measurement to the SI scale using SI transfer standards during prelaunch calibration, then performing an ongoing series of on-orbit diagnostics during its operational lifetime in space to evaluate component uncertainties. If the component uncertainties remain within the tolerances encountered during prelaunch calibration, then SI traceability can be asserted (Dykema and Anderson 2006).

Spaceborne measurements of infrared radiance can be most accurately calibrated with blackbodies. The spectral radiance $B_{\tilde{\nu}}(T)$ emitted by a blackbody cavity of uniform temperature T with an infinitesimal aperture is described by the Planck function

$$B_{\tilde{\nu}}(T) = \frac{2hc^2\tilde{\nu}^3}{\exp\left(\frac{hc\tilde{\nu}}{k_B T}\right) - 1}, \quad (1)$$

where h is Planck's constant, c is the speed of light in a vacuum, k_B is the Boltzmann constant, and $\tilde{\nu}$ is the spectral index (in cm^{-1}). The spectral radiance $I_{\tilde{\nu}}$ emitted by a cavity with a finite aperture with Lambertian reflectance is

$$I_{\tilde{\nu}} = \varepsilon_{\tilde{\nu}} B_{\tilde{\nu}}(T) + (1 - \varepsilon_{\tilde{\nu}}) B_{\tilde{\nu}}(T^{\mathrm{eff}}), \quad (2)$$

where $\varepsilon_{\tilde{\nu}}$ is the cavity emissivity and T^{eff} is the effective temperature of the radiation from the background environment assuming that it is spatially isotropic and isothermal (blackbody cavity emissivity = 1 − blackbody cavity reflectivity; the terms emissivity and reflectivity will be used in accordance with this relationship). The values of the physical constants that appear in the Planck function are known with much lower uncertainties than are required for remote sensing applications. Thus, the dominant source of uncertainty in a well-designed blackbody arises from the measurement of the cavity temperature and the effect of the nonunity emissivity of a practical blackbody with a macroscopic aperture. Demonstration of an SI-traceable infrared radiance scale requires that both blackbody temperature and emissivity be diagnosed on orbit. The SI-traceable measurement of cavity temperature on orbit was discussed in an earlier paper (Gero et al. 2008). Here, we address the on-orbit monitoring of blackbody cavity emissivity.

For satellite instruments, blackbody cavity emissivity is generally modeled numerically and/or determined experimentally during prelaunch calibration. No infrared spectrometer currently in orbit incorporates a diagnostic measurement to quantify changes in cavity emissivity over the mission lifetime. Thus, it is generally assumed, without any direct means of confirmation, that the cavity emissivity will remain constant for the duration of the mission such that Eqs. (1) and (2) will continue to apply unmodified.

The effect of exposure to the low earth orbit environment on various materials was investigated at the Long Duration Exposure Facility (LDEF). LDEF included several polyurethane paint coatings, including Aeroglaze Z306, which is the coating employed in the laboratory experiments for this paper. After 5.7 yr of space exposure, the paint surfaces underwent significant physical changes, including oxidation from atomic oxygen, paint erosion, the removal of resins, the appearance of silicate residues, cracking, and quantitative changes in optical properties (Golden 1994). The susceptibility of paint to degradation in space has thus been demonstrated. There exist, however, no diagnostics of paint optical properties of blackbodies on board the satellite instruments that rely on these properties for radiometric calibration.

In the laboratory, such painted surfaces can be characterized by reflectometry. A review of these methods and salient results are given by Persky (1999). The basic concept of reflectometry is that a light source is directed onto a sample material, and the amount of reflected light is quantified with a detector. The geometry can be such that the incident and/or reflected beam angles can be directional or the measurement may be integrated over a hemisphere.

We propose a new method to monitor blackbody emissivity on orbit using a quantum cascade laser (QCL)-based reflectometer. The QCL is a solid-state laser that can operate in continuous-wave mode at thermoelectrically cooled temperatures. The laser beam is free-space coupled into the calibration blackbody. The attenuated reflected radiation is measured with an infrared spectrometer system comprised of calibration blackbodies, an interferometer, and detectors. The QCL mass and mechanical envelope are relatively small, which facilitates integration into existing optical systems. We present a proof-of-concept experiment demonstrating the diagnostic of cavity emissivity for a blackbody with the laboratory prototype of a space-based infrared spectrometer. In the remaining sections of this paper, we describe the on-orbit reflectometry experiment in detail. In section 2, we describe the experimental apparatus, including the spectrometer, the blackbodies, and the QCL. In section 3, we discuss the experimental procedure. In section 4, we discuss the results obtained with the reflectometer. In section 5, we discuss the implications of these results for the radiometric calibration of spectrometers on orbit. We summarize our conclusions in section 6.

2. Experiment description

The experiment diagnoses an existing spectrometer system, which includes a Fourier transform spectrometer, three blackbodies, detectors, and the associated electronics. The instrument topology is similar to the Interferometer for Atmospheric Emission and Solar Absorption (INTESA) and the Scanning High-Resolution Interferometer Sounder (S-HIS; Keith et al. 2001; Revercomb et al. 2005). A QCL and a power meter are coupled into the optical system to form the reflectometer. A test blackbody was constructed to accept the QCL beam. The full apparatus is described below (illustrated in Fig. 2).

a. Spectrometer

A Bomem MR100 Fourier transform spectrometer (Bomem, Quebec, Canada) was used to obtain spectra. The MR100 is a Michelson-type interferometer with a wishbone swing arm and two input and two output ports. The spectral resolution was 0.5 cm^{-1} unapodized. It was operated with a ZnSe beamsplitter and gold-coated corner-cube retroreflectors. The modulated radiation was observed with a Kolmar KV-104 photovoltaic mercury–cadmium–telluride (MCT) detector (Newburyport, Massachusetts) with peak detectivity 9.5×10^{10} cm W^{-1} $Hz^{1/2}$ (at 10 kHz). The signal current from the detector was fed into a preamplifier (Bomem). The interferograms were produced by digitizing the preamplifier output triggered by each zero crossing of the reference He–Ne laser fringe signal emitted at 15 798 cm^{-1} (633 nm). To improve the signal-to-noise ratio, 100 interferograms were coadded before applying the Fourier transform to obtain spectra.

One of the spectrometer input ports faced a rotary table such that the spectrometer could selectively observe either one of two calibration blackbodies or the test blackbody (described in section 2c). The second input port invariably observed a reference blackbody at 25°C. The two calibration blackbodies and the reference blackbody are of identical construction. The blackbody cone, cylinder, and aperture were designed as independent interlocking aluminum modules held together using compression. This permits easy modification of the length of the cavity. A 60° reentrant cone at the base of the blackbody ensures that an incident ray undergoes a large number of specular reflections before exiting the cavity. Kapton thermofoil heaters (Minco, Minneapolis, Minnesota) are attached to each module and can be individually controlled to adjust the cavity temperature homogeneity. Because the experiment was performed at ambient pressure, convective losses were minimized by insulating the exterior of the cavity with a minimum 4-cm-thick layer of melamine and polyethylene foam. The interior surface of the cavity was sandblasted to create micron-scale roughness. The surface was primed with Aeroglaze 9947 primer and coated with Aeroglaze Z306 diffuse black paint (Lord Corp., Erie, Pennsylvania). This paint has characteristically high emissivity in the infrared low-outgassing rates and is qualified for spaceborne applications. A thin 0.06-mm coat of paint was applied to keep temperature gradients across the insulating paint to a minimum (Best et al. 2003). A measurement of the directional–hemispherical reflectance of a witness sample of the blackbody surface preparation yielded a value of 0.031 ± 0.001 (at 1264 cm^{-1}; 1σ uncertainty values are used throughout this paper). This value was used in a Monte Carlo statistical ray-tracing model (Sapritsky and Prokhorov 1992, 1995; Prokhorov 1998) to obtain an effective blackbody cavity emissivity of 0.99989.

The two calibration blackbodies were used to establish the radiance calibration of the spectrometer. They were operated at 35° and 45°C. Thermistors (Thermometrics, Edison, New Jersey) with an accuracy of 0.5 mK were used to measure the temperature of each blackbody. Using the known blackbody temperatures and cavity emissivities in the Planck function [Eqs. (1) and (2)], the spectral gain and offset parameters of the spectrometer were determined, based on the method of Revercomb et al. (1988). These parameters were then applied to the measurement of the test blackbody to obtain a calibrated spectrum. Such a two-point calibration was carried out either directly before or after each view of the test blackbody. Additional details of the spectrometer operation and blackbody design have been described elsewhere (Gero 2007; Gero et al. 2008).

b. Quantum cascade laser

Quantum cascade lasers are unipolar semiconductor lasers that exploit advances in semiconductor physics to produce high output power in the thermal infrared wavelength range. The laser is comprised of a periodic heterostructure of alternating thin layers of p- and n-doped semiconductors. After an electron undergoes a transition from a conduction band to a valence band and emits a photon in one period of the structure, it can tunnel into the next period where the process is repeated and another photon can be emitted. The process of a single electron causing the emission of multiple photons as it traverses the QCL structure leads to higher output powers than semiconductor laser diodes. A further key feature of QCLs is that the emission wavelength is primarily a function of the heterostructure layer thickness. As a consequence, QCLs can cover a wide spectral range using the same material system. QCLs are commercially available in the 600–2375-cm^{-1} range (4.2–16.7 μm; Alpes Lasers, Neuchâtel, Switzerland). Thus far, the

devices showing the best performance in this range are based on InGaAs/InAlAs alloys lattice-matched to InP.

The spectrum of the distributed feedback QCL used in the current experiment (Lucent Technologies, Murray Hill, New Jersey) is shown in Fig. 1 (top). It is sharply peaked at 1264 cm^{-1} (7.91 μm) and emits about 38 mW of power in a single mode. The QCL is mounted in a cryogenic Dewar (Kadel Engineering Corp., Danville, Indiana) and cooled to 77 K with liquid nitrogen. A ZnSe lens is positioned in front of the laser inside the Dewar to focus the beam. The laser assembly was mounted on an optical table and the beam was directed with a folding mirror to a rotary table, which could alternately position either the test blackbody or a thermopile detector to accept the beam. This permitted monitoring of the incident laser power into the test blackbody cavity. The folding mirror was mounted on a horizontal translation stage, which allowed control over the incidence point of the beam in the cavity (see Fig. 2). The laser beam had a width of 4 mm at the incidence point on the interior surface of the test blackbody.

c. Test blackbody

Although thermoelectrically cooled QCLs with greater than 100 mW of single-mode output power in the thermal infrared are readily available, the laser used in this experiment had a lower output power of 38 mW. In accordance, a test blackbody was constructed with a cavity emissivity lower than that of the blackbodies described in section 2a, such that the reflected laser signal could still be measured with adequate signal-to-noise resolution. A diagram of the cavity is shown in Fig. 2, and the cavity's physical parameters are listed in Table 1. The test blackbody was operated at 40°C for all experiments.

The test blackbody employs the same design as the calibration and reference blackbodies (described in section 2a). The main difference between them is that the test blackbody is built with one cylindrical module, has a length of 91 mm, and a modeled effective emissivity of 0.999 55, whereas the calibration and reference blackbodies are built with three cylindrical modules, are 244 mm long, and have an effective emissivity of 0.999 89. In addition, the test blackbody has a tapered cone facing away from the aperture, whereas the calibration and reference blackbodies employ a reentrant cone that faces toward the aperture.

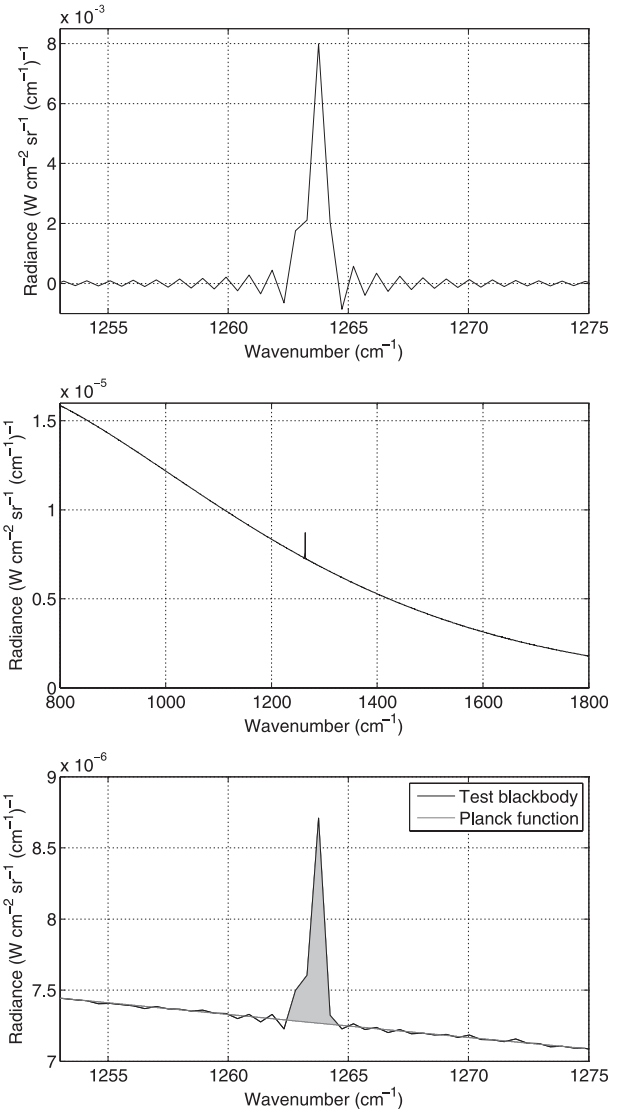

FIG. 1. (top) Spectrum of the QCL homogenized in a reflective cavity and observed with a Fourier transform spectrometer at 0.5 cm^{-1} resolution (unapodized). The oscillations in the spectrum resembling a sinc function arise from the finite optical path difference of the interferometer. (middle) Spectrum of the test blackbody as observed by the spectrometer, which shows the sharp laser peak superimposed on the baseline blackbody radiation at 40°C. (bottom) Expanded view of the laser peak in (middle) (dark curve). The lighter curve is the fitted-baseline Planck function. The shaded area between the peak and the baseline fit represents the reflected laser radiance $I_{\text{reflected}}^{\text{laser}}$.

3. Methodology

The goal of this experiment was to determine the amount of the incident laser power that is reflected from the cavity and furthermore to evaluate whether this quantity is sensitive to small perturbations in the incidence point of the laser on the blackbody interior. Calibrated measurements were made of the radiance of the test blackbody illuminated with the QCL. For this procedure, the QCL was first turned on and allowed to stabilize, and the power in the laser beam was measured

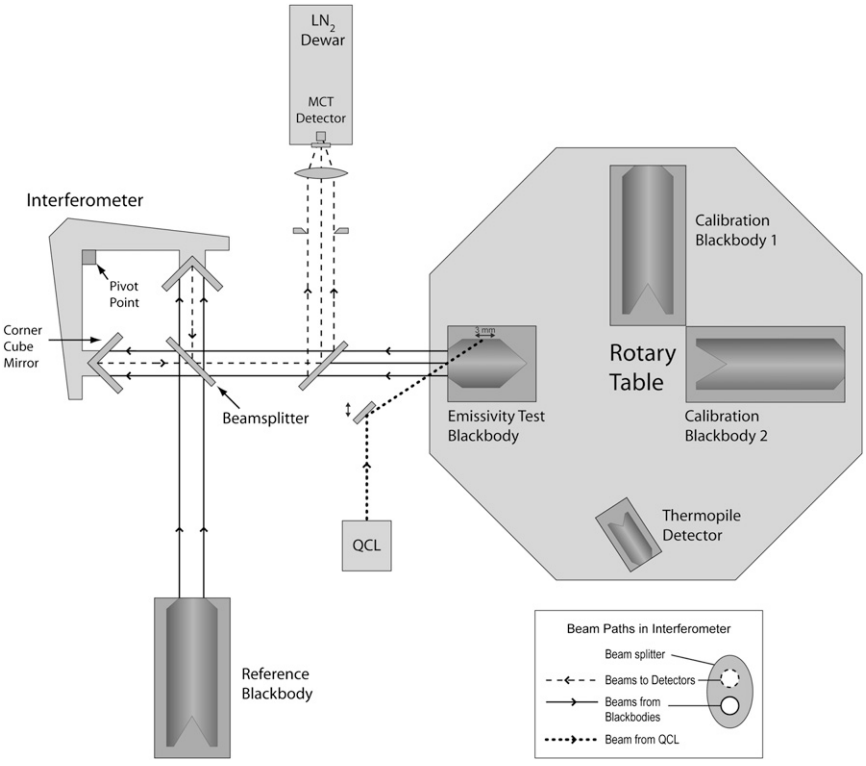

FIG. 2. Experimental layout showing the spectrometer, blackbodies, detectors, and the reflectometer subsystem. The rotary table can be moved to position the appropriate targets in line with the spectrometer and the QCL. The QCL beam is directed into the test blackbody cavity using a folding mirror that lies outside of the field of view of the spectrometer. The diameter of the laser beam is 4 mm at the point of incidence on the cavity. The beam was steered over a distance of 3 mm along the interior surface of the cavity by translating the folding mirror (indicated by arrows; not to scale).

using the thermopile detector. Then, the beam was directed into the test blackbody and its spectrum was observed using the spectrometer. Afterward, the laser beam power was measured again. This was followed by views of each of the two calibration blackbodies to determine the calibration coefficients. Then the test blackbody was observed again with measurements of the illuminating laser beam power preceding and following the measurement as before. This cycle of four blackbody views by the spectrometer and laser power monitoring was repeated multiple times at various positions of the incident laser beam. The incidence point of the beam was varied over a length of 3 mm measured along the central symmetry axis of the cavity and sampled at 0.75-mm intervals (the geometry is depicted in Fig. 2). A minimum of six calibrated measurements were made at each position, and the results were averaged. The experiment was performed at room temperature and pressure. The entire apparatus was operated inside a purge box under a constant flux of nitrogen gas to reduce contamination in the spectra from water vapor and to stabilize the ambient temperature.

4. Results and analysis

Figure 3 (top) shows the average incident laser power $P_{\text{incident}}^{\text{laser}}$, which was recorded for various horizontal positions of laser beam incidence along the interior of the cavity. The error bars show the random uncertainty (type A) associated with the measurement, which is listed in Table 1. The systematic uncertainty (type B) of the thermopile detector is 10%. The systematic uncertainty is not propagated in the uncertainty analysis for laser reflectivity because this uncertainty will not be present in the envisioned flight configuration, as discussed in section 5. Within the random uncertainty of the measurement, there is no significant variation in incident laser power at various horizontal positions throughout the entire experiment.

Figure 1 (middle) shows a calibrated spectrum of the test blackbody illuminated by the QCL. The two components are clearly visible: a baseline of Planck blackbody radiation from a 40°C blackbody and a superimposed peak from the QCL. Figure 1 (bottom) shows an

TABLE 1. List of experimental parameters and results. All uncertainties are 1σ values.

Component	Value	Unit
Test blackbody		
Length	91.4	mm
Aperture diameter	38.1	mm
Aperture area	11.4	cm^2
Aperture solid angle	2π	sr
Measured surface reflectivity at 1264 cm^{-1}	0.031	—
Modeled cavity reflectivity at 1264 cm^{-1}	4.5×10^{-4}	—
Incident laser power		
Mean	3.84×10^{-2}	W
Mean random uncertainty	1.7×10^{-4}	W
Systematic uncertainty	3.8×10^{-3}	W
Reflected laser power		
Mean	3.54×10^{-5}	W
Spectral-noise random uncertainty	6.0×10^{-7}	W
Spectral-scale random uncertainty	3.4×10^{-6}	W
Positional dependence	-3.6×10^{-6}	W mm^{-1}
Laser reflectivity		
Mean	9.22×10^{-4}	—
Mean random uncertainty	8.9×10^{-5}	—
Positional dependence	-9.5×10^{-5}	mm^{-1}

expanded view of the laser peak. To determine the reflected laser power, the area under the laser peak that is above the blackbody baseline is calculated. For this procedure, first the baseline is calculated by fitting a Planck function to the spectra on a 100-cm^{-1} interval, 50 cm^{-1} away from the center of the laser peak. Then, the area under the central peak above the baseline is numerically evaluated. This yields a radiance value $I^{\text{laser}}_{\text{reflected}}$ (in units of W cm^{-2} sr^{-1}). The power P emitted by a Lambertian source, such as a blackbody, is given by

$$P = \int_A dA \int_\Omega I \cos\theta \, d\Omega, \tag{3}$$

where A is the area of the aperture, I is the radiance, θ is the zenith angle to the surface normal, and Ω is the solid angle. For the current geometry, assuming that the reflected laser radiation has a Lambertian distribution from the blackbody aperture into a hemisphere, we have

$$P^{\text{laser}}_{\text{reflected}} = \pi A I^{\text{laser}}_{\text{reflected}}, \tag{4}$$

where A is the area of the blackbody aperture listed in Table 1. The validity of the Lambertian assumption is discussed in section 5. The laser reflectivity ρ^{laser} by the cavity for a particular illumination geometry is then given by

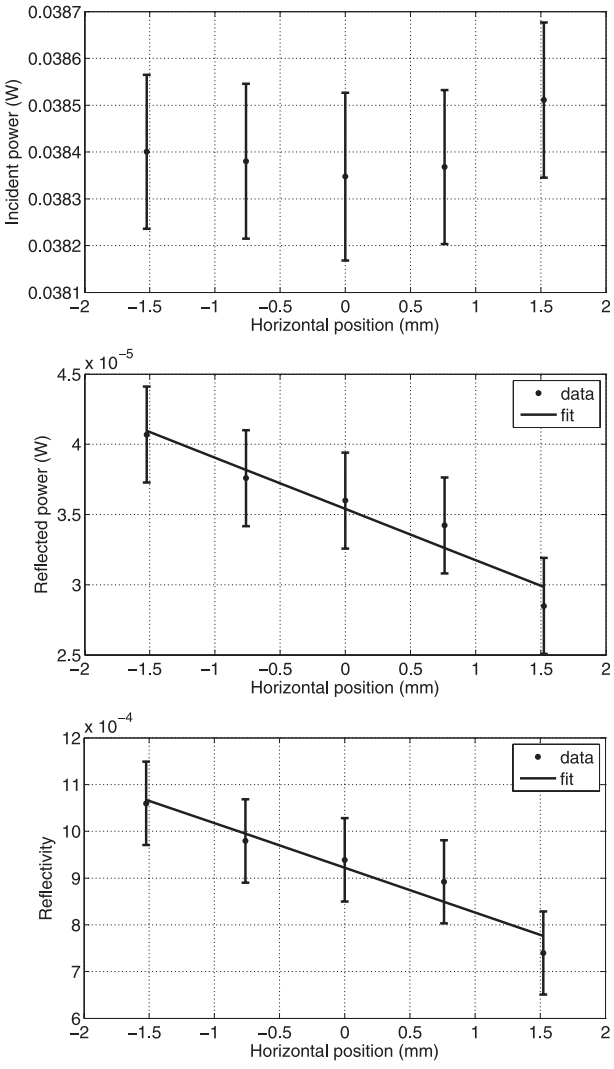

FIG. 3. (top) Incident power $P^{\text{laser}}_{\text{incident}}$ of the QCL, as measured with the thermopile detector, when the beam was aimed at different horizontal positions along the interior surface of the blackbody cavity. (middle) Reflected laser power $P^{\text{laser}}_{\text{reflected}}$ as a function of horizontal position. The solid line is the least squares fit to the measurements and has a slope of -3.6×10^{-6} W mm^{-1}. (bottom) Laser reflectivity ρ^{laser} in the test blackbody cavity as a function of horizontal position. The solid line is the least squares fit to the measurements and has a slope of -9.5×10^{-5} mm^{-1}. (top)–(bottom) Error bars represent the 1σ random uncertainty.

$$\rho^{\text{laser}} = \frac{P^{\text{laser}}_{\text{reflected}}}{P^{\text{laser}}_{\text{incident}}}. \tag{5}$$

Figure 3 (middle and bottom) shows the reflected laser power and the laser reflectivity as a function of horizontal position. There are two main sources of random uncertainty (type A) in the calculation of reflected laser power. The first is spectral noise in the baseline

blackbody radiation. This can be characterized by the variance in measurements of reflected power for a given horizontal beam position for a given experimental run. The second source of uncertainty arises from the repeatability of the spectrometer spectral scale. Each time the spectrometer is initialized, a new spectral scale is established based on the location of the point of zero path difference between the two interferometer arms. Because of the relatively coarse spectral resolution of the spectrometer (0.5 cm^{-1}) with respect to the width of the laser peak, small variations in the spectral scale can lead to errors in the determination of the area under the laser peak. The root-sum-of-squares systematic uncertainty (type B) of the spectrometer subsystem (including thermometry, blackbodies, stray light, and detector chain nonlinearity) is estimated to be 41 mK in radiance temperature, or 0.08% of the blackbody radiance at 1264 cm^{-1} at 40°C (Anderson et al. 2004; Gero 2007). The systematic uncertainty is not propagated in the uncertainty analysis for laser reflectivity, as further discussed in section 5. The magnitude of the random uncertainties and the mean results are listed in Table 1.

5. Discussion

The reflected laser power from the test blackbody was successfully detected and measured with the spectrometer. The method of determining reflected laser power by computing the area under the laser peak in the calibrated spectrum is robust. The repeatability in this measurement over the course of an experimental run (spectral-noise random uncertainty) is 1.7%. The day-to-day repeatability (spectral-scale random uncertainty) affected by the reinitialization of the spectrometer spectral scale is 9.5%.

The free-space coupling of the laser beam into the blackbody cavity was successfully demonstrated. The beam was steered over a distance of 3 mm along the interior surface of the cavity. The reflected laser power exhibited a dependence on the position of the incident laser beam along the cavity interior surface. Figure 3 (middle) shows the linear least squares fit to the observed reflected laser power, which has a positional dependence of -3.6×10^{-6} W mm^{-1} over the area under study. Similarly, the laser reflectivity exhibited a positional dependence of -9.5×10^{-5} mm^{-1}, as shown in Fig. 3 (bottom). The incident QCL laser power was steady within the measurement uncertainty over the course of the experiments; therefore, changes in the laser reflectivity are attributable to changes in reflected laser power, which is a function of the cavity geometry. The overall random uncertainty (type A) in the measurement of laser reflectivity is 8.9×10^{-5}, or 9.7% of the mean reflectivity.

These results are encouraging that a QCL-based reflectometer can be deployed on satellite instruments to monitor cavity emissivity. The measured mean laser reflectivity for the test blackbody was 9.22×10^{-4}. This is a factor of 2 larger than the modeled cavity reflectivity of 4.5×10^{-4}. This diagnostic, however, does not specifically measure the absolute reflectivity of the blackbody cavity. Because of the primarily diffuse reflectance characteristics of the Aeroglaze paint, the incident laser beam is reflected multiple times in many directions within the blackbody before exiting the cavity. If a sufficient number of reflections occur within the cavity, then the laser reflectivity ρ^{laser} can be a suitable proxy for effective cavity reflectivity; that is, if the laser reflectivity does not significantly vary over a time interval on orbit, then the effective cavity reflectivity also has not changed significantly. A likely cause of the discrepancy between the measured laser reflectivity and the modeled cavity reflectivity is the assumption in the conversion of laser radiance to power [in Eq. (3)] that the reflected laser radiation exiting the blackbody aperture is Lambertian. If the laser beam is not reflected a sufficient number of times inside the cavity, then the Lambertian assumption does not hold. If a large fraction of the reflected laser beam is directed into the field of view of the spectrometer after only a few internal reflections, then the spectrometer would observe a higher laser radiance than expected for a Lambertian source. A geometrical correction factor to Eq. (3) may bring the measured and modeled results into closer agreement. This hypothesis will be investigated, and a better physical understanding of the quantity ρ^{laser} can be gained with Monte Carlo modeling (Prokhorov et al. 2007). Using the laser and blackbody geometries, a full bidirectional reflectance distribution function (BRDF) of the blackbody surface preparation, and the spectrometer viewing geometry, a realistic model can be created that relates the laser reflectivity to the effective cavity reflectivity. This work will be presented in a future paper.

The computation of laser reflectivity requires that the measurement of laser power be normalized; in this case, we used a thermopile detector. Having a separate detector for normalization introduces additional uncertainty into the measurement. In particular, the sensitivity of this detector may drift with time on a satellite instrument in the space environment. If the uncertainty of the QCL-based reflectometer was to approach or exceed the expected drift in cavity reflectivity, then interpretation of the diagnostic would become ambiguous. This problem can be overcome by using the same detector for both normalization and the reflectivity measurement. The QCL can be directed onto a reflective

target that is known to be optically stable in the space environment. The reflected radiance from this target (e.g., Fig. 1, top) can then be used to normalize the measurement of reflected laser power from the blackbody cavity. This would eliminate the need for a second detector and the associated uncertainty from the measurement. The ratiometric measurement scheme would also reduce some of the systematic errors from the spectrometer subsystem. This mode of operation of the reflectometer will not provide an absolute measurement of laser reflectivity, but it can quantify relative drifts in effective blackbody emissivity over time with respect to an optically stable reference target. With this relative measurement mode of operation in mind, only the random uncertainties (type A) are used in the uncertainty analysis for laser reflectivity in the current experiment.

The measured laser reflectivity exhibits a dependence on the incidence point of the beam within the cavity. Thus, it is critical that the laser optics be physically secured in a way that the position of the incidence point varies less then the equivalent measurement uncertainty in laser reflectivity. From Fig. 3 (bottom), an uncertainty in reflectivity better than 8.9×10^{-5} corresponds to a pointing accuracy of better than 0.9 mm along the blackbody cavity surface. Furthermore, Monte Carlo modeling of the blackbody–QCL optical system can identify optimal incidence geometries of the laser beam inside the cavity to minimize sensitivity in laser reflectivity due to perturbations in incidence position.

In this experiment, a test blackbody cavity with an effective emissivity of 0.999 55 was used to obtain a sufficient amount of reflected laser power from a 38-mW incident laser beam. Distributed feedback QCLs producing more than 100 mW of power in a single mode in the thermal infrared are commercially available (Alpes Lasers). With such a laser, a blackbody cavity with effective emissivity of 0.999 83 could be monitored with the same signal-to-noise ratio as in the current experiment.

The possibility exists that on-orbit changes in the optical properties of the blackbody surface preparation will have spectral dependence. Although QCLs are commercially available in the 600–2375-cm^{-1} range, a single laser is tunable only over a narrow ($\sim$3 cm^{-1}) spectral range. The diagnostic capability of this method can be extended by employing multiple QCLs operating at various wavelengths. The operation of QCL arrays, built on a single substrate but each lasing at a different wavelength, has been demonstrated (Wittmann et al. 2006). Thus, monitoring cavity emissivity over a broad spectral range could be accomplished with a single thermoelectrically cooled package.

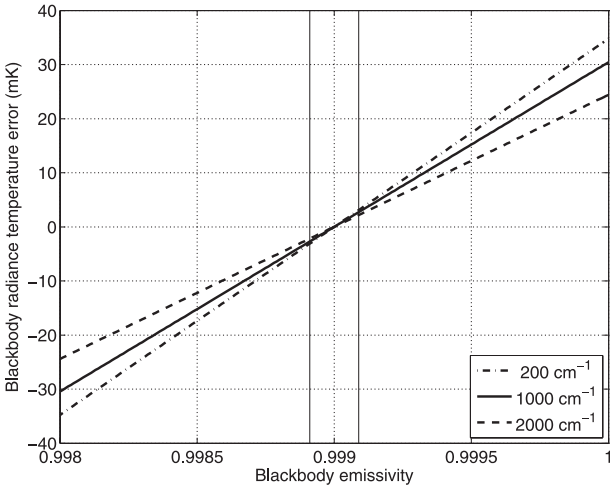

FIG. 4. Error in the calculation of blackbody radiance temperature arising from an uncorrected change in blackbody cavity effective emissivity. The horizontal axis indicates the value of uncorrected drifted cavity effective emissivity from the initial value of 0.999. The vertical axis shows the corresponding error in the calculation of blackbody radiance temperature based on the uncorrected value of cavity effective emissivity. The calculation is for a blackbody at 330 K. Results are shown at 200, 1000, and 2000 cm^{-1} for the same error in emissivity. The solid vertical lines represent the random uncertainty (type A) in emissivity measurement achieved in the current experiment.

The impact of blackbody emissivity change on calibration accuracy can be illustrated using a simple model based on Eqs. (1) and (2). The true radiance from a calibration blackbody can be obtained by solving Eq. (2) for $B_{\tilde{\nu}}(T)$, given a measurement of the apparent radiance $I_{\tilde{\nu}}$ and knowledge of the parameters $\varepsilon_{\tilde{\nu}}$ and T^{eff}. Figure 4 shows the component of error in the calculation of blackbody radiance arising from incorrect knowledge of $\varepsilon_{\tilde{\nu}}$. Figure 5 shows the change in total combined instrument uncertainty resulting from cavity emissivity drift for a high-accuracy infrared spectrometer satellite instrument. The results indicate that a drift in cavity emissivity of 8.9×10^{-5}, which is detectable with the current experimental setup, corresponds to blackbody radiance temperature errors of 2.2, 2.7, and 3.1 mK at 2000, 1000, and 200 cm^{-1}, respectively. These detection limits are well below the current accuracies of infrared sounders.

6. Conclusions

An in situ reflectometer was implemented and used to monitor the reflectivity of a blackbody cavity within an infrared spectrometer instrument. The reflectometer was designed to have a small mechanical envelope so that it can be readily incorporated into satellite instrument designs. The reflectometer employed a quantum

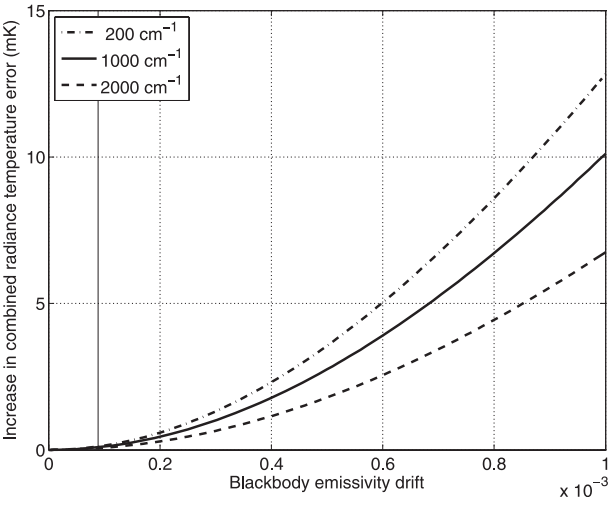

FIG. 5. Change in total combined instrument uncertainty arising from a drift in cavity emissivity. The horizontal axis indicates the magnitude of uncorrected drift in cavity effective emissivity from an initial value of 0.999 for a cavity operating at 330 K, as in Fig. 4. The combined uncertainty estimate is comprised of the root-sum-of-squares uncertainties from an estimate of the system-level error budget of a proposed high-accuracy infrared spectrometer satellite instrument (Anderson et al. 2004; Gero 2007), which includes uncertainties from thermometry, blackbodies, stray light, polarization, detector chain nonlinearity, and emissivity drift. The solid vertical line represents the random uncertainty (type A) in emissivity measurements achieved in the current experiment.

cascade laser operating at 1264 cm^{-1} (7.91 μm) emitting 38 mW of power in a single mode. The mean laser reflectivity within a test blackbody cavity was measured to be 9.22×10^{-4} with an uncertainty of 8.9×10^{-5}. These results suggest that a refined version of this reflectometer has the potential to be deployed on a satellite infrared sounder to monitor changes in onboard blackbody emissivity on scales finer than the current levels of radiometric accuracy. The QCL-based reflectometer is versatile and can be adapted to monitor blackbodies with various geometries, temperatures, and diffuse surface coatings over a broad range of frequencies in the thermal infrared. Implementation of this diagnostic tool can lead to improved radiometric accuracy, as any drift in blackbody emissivity needs to be evaluated on orbit to physically justify the use of the Planck function in the determination of blackbody radiance. This diagnostic of blackbody emissivity could facilitate an SI-traceable measurement of infrared radiance from space.

Acknowledgments. The authors acknowledge the engineering support of L. Lapson, M. Greenberg, C. Tuozzolo, J. Demusz, M. Rivero, and T. Martin, as well as technical insight from M. Witinski and H. Revercomb.

REFERENCES

Anderson, J. G., J. A. Dykema, R. M. Goody, H. Hu, and D. B. Kirk-Davidoff, 2004: Absolute, spectrally-resolved, thermal radiance: A benchmark for climate monitoring from space. *J. Quant. Spectrosc. Radiat. Transfer,* **85,** 367–383.

Best, F. A., and Coauthors, 2003: Traceability of absolute radiometric calibration for the Atmospheric Emitted Radiance Interferometer (AERI). *Proc. Characterization and Radiometric Calibration for Remote Sensing,* Logan, UT, Space Dynamics Laboratory, CD-ROM.

Dykema, J. A., and J. G. Anderson, 2006: A methodology for obtaining on-orbit SI-traceable spectral radiance measurements in the thermal infrared. *Metrologia,* **43,** 287–293.

Gero, P. J., 2007: Realization of SI-traceable infrared radiance measurements from space for achieving benchmark climate observations. Ph.D. dissertation, Harvard University, 133 pp.

——, J. A. Dykema, and J. G. Anderson, 2008: A blackbody design for SI-traceable radiometry for earth observation. *J. Atmos. Oceanic Technol.,* **25,** 2046–2054.

Golden, J. L., 1994: Results of the examination of LDEF polyurethane thermal control coatings. NASA Contractor Rep. 4617, 141 pp.

Keith, D. W., J. A. Dykema, H. Hu, L. Lapson, and J. G. Anderson, 2001: Airborne interferometer for atmospheric emission and solar absorption. *Appl. Opt.,* **40,** 5463–5473.

Leroy, S. S., J. G. Anderson, and G. Ohring, 2008: Climate signal detection times and constraints on climate benchmark accuracy requirements. *J. Climate,* **21,** 841–846.

National Research Council, 2007: *Earth Science and Applications from Space: National Imperatives for the Next Decade and Beyond*. National Academies Press, 456 pp.

Ohring, G., Ed., 2008: *Achieving Satellite Instrument Calibration for Climate Change*. U.S. Dept. of Commerce, 144 pp.

Persky, M. J., 1999: Review of black surfaces for space-borne infrared systems. *Rev. Sci. Instrum.,* **70,** 2193–2217.

Prokhorov, A. V., 1998: Monte Carlo method in optical radiometry. *Metrologia,* **35,** 465–471.

——, S. N. Mekhontsev, and L. M. Hanssen, 2007: Radiative properties of blackbody calibration sources: Recent advances in computer modeling. *Int. J. Thermophys.,* **28,** 2128–2144.

Revercomb, H. E., H. Buijs, H. B. Howell, D. D. LaPorte, W. L. Smith, and L. A. Sromovsky, 1988: Radiometric calibration of IR Fourier transform spectrometers: Solution to a problem with the High-Resolution Interferometer Sounder. *Appl. Opt.,* **27,** 3210–3218.

——, and Coauthors, 2005: Highly accurate FTIR observations from the scanning HIS aircraft instrument. *Multispectral and Hyperspectral Remote Sensing Instruments and Applications II,* A. M. Larar, M. Suzuki, and Q. Tong, Eds., International Society for Optical Engineering (SPIE Proceedings, Vol. 5655), 41–53.

Sapritsky, V. I., and A. V. Prokhorov, 1992: Calculation of the effective emissivities of specular-diffuse cavities by the Monte Carlo method. *Metrologia,* **29,** 9–14.

——, and ——, 1995: Spectral effective emissivities of nonisothermal cavities calculated by the Monte Carlo method. *Appl. Opt.,* **34,** 5645–5652.

Wittmann, A., M. Giovannini, J. Faist, L. Hvozdara, S. Blaser, D. Hofstetter, and E. Gini, 2006: Room temperature, continuous-wave operation of distributed feedback quantum cascade lasers with widely spaced operation frequencies. *Appl. Phys. Lett.,* **89,** 141116, doi:10.1063/1.2358939.